Supplementary Materials and Methods

Cell culture

The ST-*Hdh*$^{Q7/Q7}$ and ST-*Hdh*$^{Q111/Q111}$ were kindly provided by M.E MacDonald, and were cultured as previously described *(S1)*. Neuro2A cells were obtained from ATCC and grown at 37C° in DMEM supplemented with 2 mM of L-Glutamine and 10% FBS. Neuron differentiation was induced by substituting all-trans retinoic acid (Sigma; St. Louis, MO) for DMEM for 24 hrs. Hydrogen peroxide treatment was performed by adding hydrogen peroxide to this media at the stipulated concentrations for 4 hrs. Quantification of aggregation was performed by counting the number of RFP-positive cells in the field with punctate GFP staining, and dividing by the total number of cells in the field. For each experiment, we analyzed at least 60 cells in at least four sections, and all experiments were performed independently by two different observers in triplicate or quadruplicate. Analysis of cell death with activated caspase-3 was performed as previously described *(S2)*. Induction of lysosomal stress was achieved by treating Neuro2a cells with 100 mM sucrose for 48 hrs. In all experiments, the investigator was blinded to culture conditions or cell treatments.

Real-time RT-PCR analysis

Total RNAs were isolated with the Qiagen RNeasy Lipid tissue extraction kit (Qiagen, Valencia, CA). Genomic DNA was removed using RNAse free DNAse (Ambion; Austin, TX). Quantification of mRNA was performed using an Applied Biosystems 7500 Real Time Sequence Detection System with ABI Assays-on-Demand primers and TaqMan® based probes *(S3)*. ABI TaqMan primer and probe set designations are available upon request. 18S RNA was used as the

internal control to normalize results. Relative expression levels were calculated via the Standard Curve method *(S4)*.

Luciferase assay

We transfected the TFEB promoter-reporter luciferase construct and pRL-CMV (Promega) with or without the PGC-1α expression vector into Neuro2A cells or ST-*Hdh* cells. Cells were harvested 24 hrs after transfection and then subjected to luminescence detection by performing dual luciferase assays using the Dual-Luciferase® Reporter Assay system (Promega). For luminescence measurement, we used Perkin Elmer VICTOR X Light (Perkin Elmer; Waltham, MA), and we used *Renilla* luciferase activity for normalization.

Western and dot blot analysis

Protein lysates from striatum were prepared as previously described *(S5)*. We loaded 20 μg of homogenized proteins per lane, and after running 10% Bis-Tris gels (Invitrogen), samples were transferred to PVDF membranes (Millipore), which were blocked in 3% PBS with 0.1% Tween20 (PBS-T) at RT for 1 hr. Membranes were incubated with cathepsin-D antibody (sc-6486; Santa Cruz) or 1C2 antibody (MAB1574; Millipore) in PBS-T with 3% BSA at 4°C overnight. The primary antibody was visualized with horseradish-peroxidase conjugated anti-mouse IgG (Santa Cruz) at 1:10,000 dilution and Enhanced Chemiluminescence (Amersham). We performed dot blot analysis as previously described *(S6)*, but with minor modifications. Briefly, we prepared 1 μg of homogenized striatum and resuspended the lysates in 1 ml of PBS with 0.01% Tween20 (PBS-T2). After applying the sample to nitrocellulose membranes, membranes were washed with PBS-T2, and then were incubated in 10% non-fat dried milk in

PBS-T at 4°C overnight. Membranes were incubated with affinity-purified anti-oligomer antibody A11 at 1:2,000 dilution or anti-fibril antibody OC at 1:10,000 dilution in PBS-T2 with 3% BSA at RT for 1 hr. Primary antibody signals were visualized as described above.

Mitochondrial studies

We measured mitochondria complex I and II activities in mouse striatum, as previously described *(S7)*. For measurement of adenine nucleotides, ATP, ADP, AMP, and adenosine present in TCA extracts from the striatum and cortex were quantitatively converted to fluorescent 1,N^6-ethenoadenine derivatives as previously described *(S8)*. For quantification of mitochondrial DNA copy number, real-time DNA PCR analysis was performed with the NovaQUANT™ Mouse Mitochondrial Biogenesis qPCR Kit (Novagen), according to the manufacturer's instructions.

Oxidative damage and oxidative stress experiments

For detection of carbonyl groups, we employed the OxyBlot™ Protein Oxidation Detection Kit (Millepore, Billerica, MA). Briefly, we prepared 20 μg of homogenized striatum / individual mouse, and divided the samples for derivatization and for the control reaction. After 15 min incubation, we added 7.5 μl of neutralization solution to stop the reaction. Treated samples and negative controls were alternately loaded onto 12% polyacrylamide gels (Invitrogen). To detect 4-hydroxynonenal (4-HNE), we immunoblotted 20 μg striatum lysates with a rabbit anti-4-HNE antibody, according to the manufacturer's directions (Millipore). We measured Thiobarbituric Acid Reactive Substances (TBARS) using the TBARS assay (Cayman, Ann Arbor, MI), and performed 8-hydroxy-2-deoxyguanosine quantification, using an EIA assay (Cayman, Ann

Arbor, MI). For reading spectrophotometric absorbances in these two assays, we used our VersaMax microplate reader (Molecular Devices, Sunnyvale, CA). All studies of *in vivo* oxidative damage were performed on cohorts of ≥ 3 mice / group, and repeated in triplicate.

We transfected RFP-PGC-1α or RFP-empty vector into ST-*Hdh* cells and 24 hrs after transfection, we changed the media to expose the cells to various concentrations of hydrogen peroxide for 4 hrs. N-acetyl cysteine was added to achieve a final concentration of 5 mM. To quantify ROS levels, we exposed cells to a thiol-reactive chloromethyl group by culturing the cells for 30 min in media containing 20 μM CM-H2DCFDA (Invitrogen). Fluorescence imaging was performed with a Marianas™ imaging system (Intelligent Imaging Innovations; Denver, CO), consisting of a CoolSnap HQ camera (Photometrics; Tuscon, AZ), Zeiss Axiovert 200M inverted microscope, and a liquid light guide coupled 175W Xenon lamp (Sutter Instrument Co., Novato, CA) controlled by Slidebook™ 5.0 software (Intelligent Imaging Innovations; Denver, CO). We measured GFP fluoro-intensity in RFP-positive cells, and calculated fluoro-intensities by averaging the measurements from 50 different cells.

Chromatin Immunoprecipitation assay

We performed chromatin immunoprecipitation (ChIP) as previously described *(S9)*. Briefly, we transfected Neuro2A cells with a PGC-1α expression construct, and 24 hrs after transfection, we treated cells for 10 min with 1% formaldehyde. After sonication, lysates were incubated with anti-PGC-1 α antibody (H-300, Santa Cruz Biotechnology) or control rabbit IgG (Santa Cruz Biotechnology) overnight at 4°C. Quantitative PCR analysis was performed with the SYBR-GREEN PCR master Mix (ABI) on a 7500 Sequence Detection System (ABI). Primer sequences

used for ChIP are available upon request.

Chymotrypsin-like activity

We measured chymotrypsin-like activity in Neuro2A cells, either transfected with PGC-1α or treated with NAC. After 24 hrs, we added hydrogen peroxide at specified concentrations for 4 hrs, harvested cells, and homogenized in 200 μl of buffer (50 mM Tris–HCl, pH 7.5, 250 mM sucrose, 5 mM $MgCl_2$, 0.5 mM EDTA), containing 2 mM ATP, 1 mM DTT, and 0.025% digitonin. We incubated resuspended cells on ice for 5 min, centrifuged at 13,000 rpm for 15 min at 4°C, and then transferred the supernatant. 50 μg of protein was added to a 96-well plate to which we added 100 μl of assay buffer, containing Suc-Leu-Leu-Val-Tyr-AMC (LLVY) at 200 μM concentration. Enzyme activity was assayed by recording fluorescence activity at 37°C every 5 min over 1 hr, with excitation and emission wavelengths of 380 and 460 nm respectively.

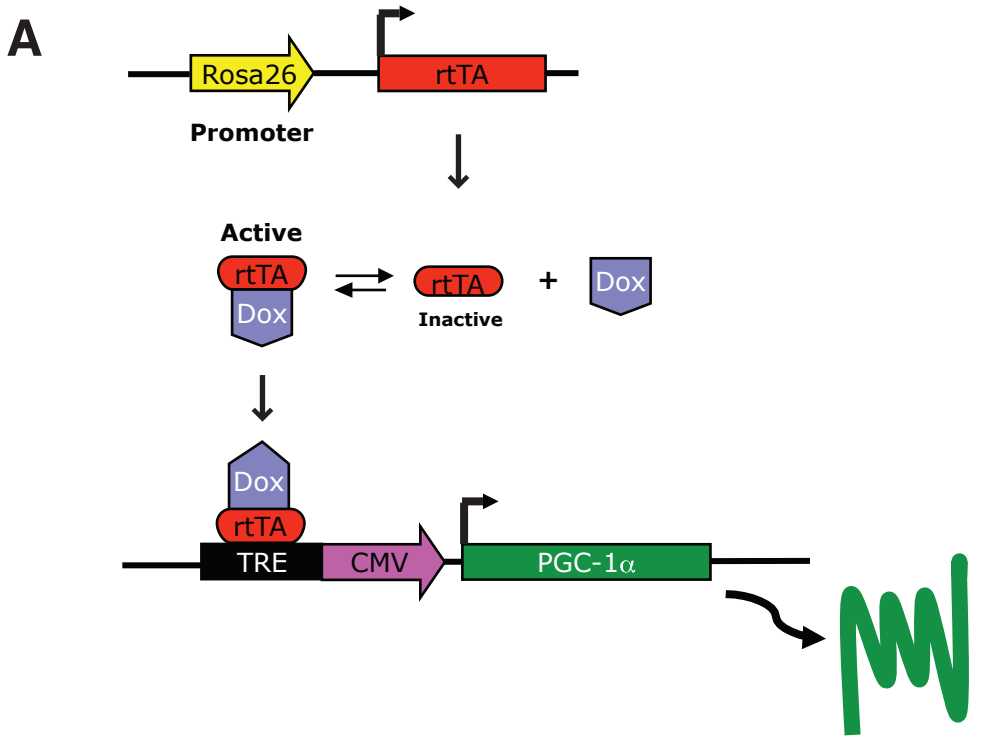

B

Rosa26-rtTA	; TRE-PGC-1α	x HD-82Q; Rosa26-rtTA	
↓			
HD-82Q	; -	; Rosa26-rtTA	(HD)
HD-82Q	; TRE-PGC-1α	; -	(HD)
HD-82Q	; TRE-PGC-1α	; Rosa26-rtTA	(triple)
-	; TRE-PGC- 1α	; Rosa26-rtTA	(control)
-	; TRE-PGC- 1α	; -	(control)
-	; -	; Rosa26-rtTA	(control)
-	; -	; -	(WT)

Figure S1. Induction of PGC-1α expression in transgenic mice

A) Our method for induction of PGC-1α expression relies upon the production of bigenic mice that carry the Rosa26 locus modified to contain the reverse tetracycline trans-activator (rtTA) gene (top), and also contain a PGC-1α transgene (bottom), driven by a minimal CMV promoter linked to a tetracycline response element (TRE). The CMV promoter drives ubiquitous expression, while Rosa26 promoter drives expression in almost all cell types, including neurons, but is notoriously poor for driving expression in cells of the astroglial lineage *(S10)*. When bigenic mice receive doxycycline (Dox), the rtTA becomes activated upon Dox binding, and then the Dox-rtTA complex associates with the TRE to promote the expression of PGC-1α.
B) To obtain a set of three cohorts (HD, triple, and control), we crossed bigenic Rosa26-rtTA; TRE- PGC-1α mice with HD-N171-82Q; Rosa26-rtTA mice, after crossing all lines of mice onto the C57BL/6J background. This cross yielded seven different genetic combinations, two of which serve as the "HD" cohort, and four of which serve as the "control" cohort. Only mice that are "triple" transgenic for HD-82Q, TRE-PGC-1α, and Rosa26-rtTA will respond to doxycycline to induce significant expression of PGC-1α.

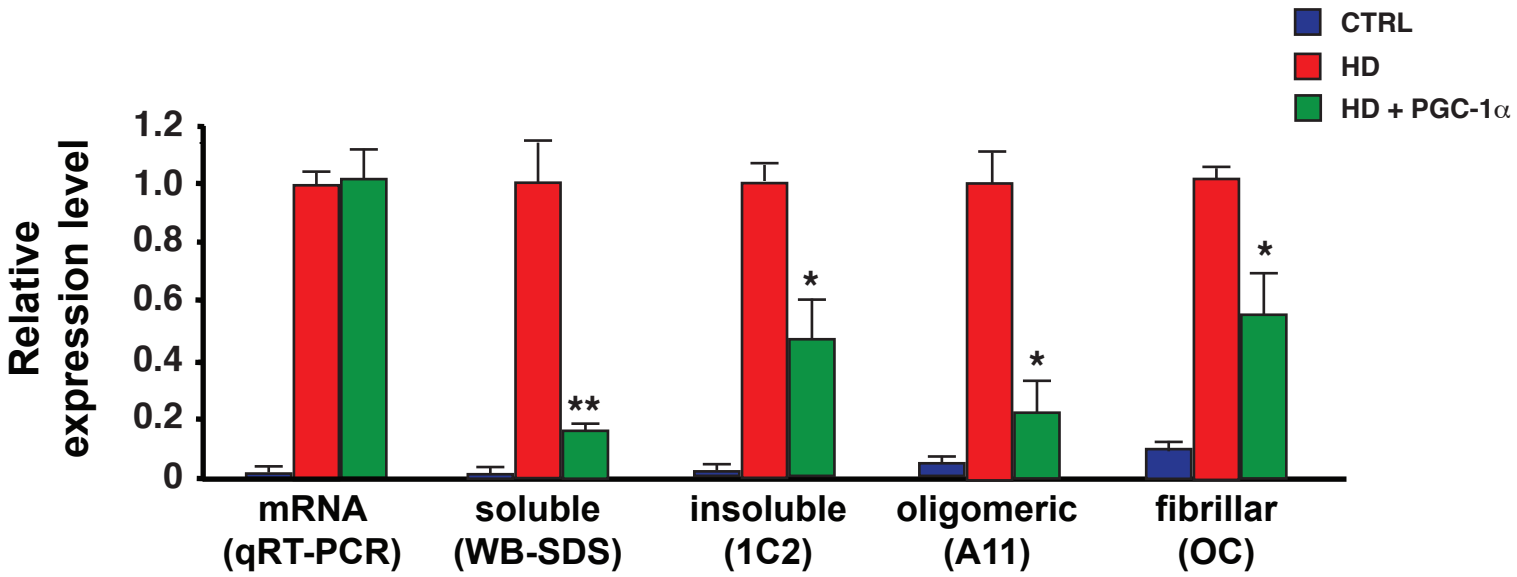

Figure S2. Effect of PGC-1α over-expression on htt RNA and protein expression

We performed a series of experiments on striatal RNAs or protein lysates isolated from 13 week-old cohorts (n = 4 – 6 / group) of non-HD controls (CTRL), HD N171-82Q mice (HD), and HD N171-82Q mice induced to express PGC-1α (HD + PGC-1α). Here we see the quantitative read-outs for qRT-PCR, SDS-PAGE Western blot analysis of soluble htt protein, and filter trap analysis of htt protein with three different antibodies that detect different species of misfolded htt protein. In all cases, results are normalized to HD mice whose values are arbitrarily set to 1.0. HD mice and HD mice induced to express PGC-1α exhibit identical levels of htt transgene mRNA. However, soluble htt protein, insoluble htt protein, oligomeric htt protein, and fibrillar htt protein levels are all significantly decreased in HD N171-82Q mice induced to express PGC-1α (* $P < .05$; ** $P < .01$). Error bars = s.e.m.

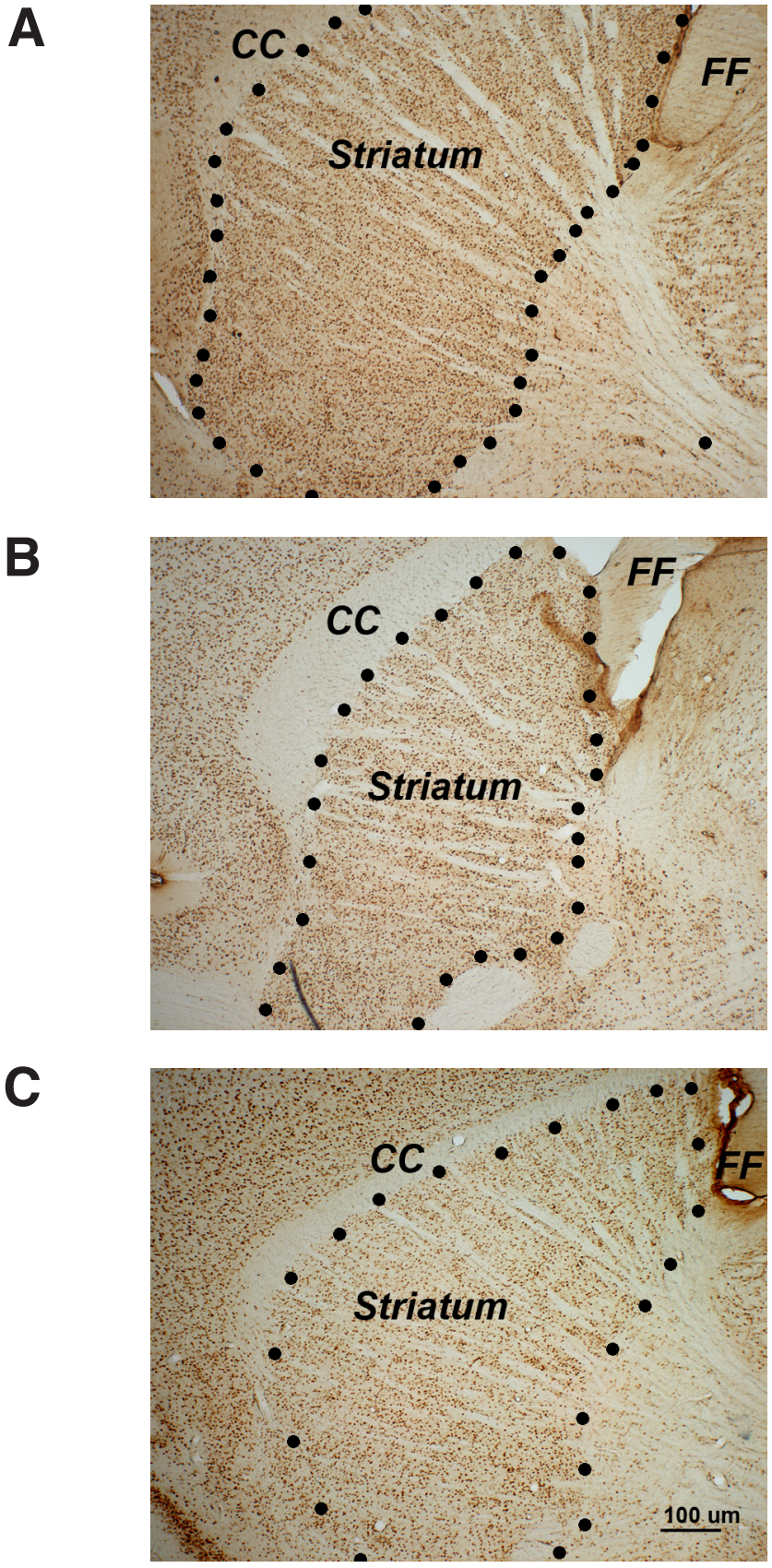

Figure S3. Representative striatal sections for stereology analysis

Here we see representative images from 18 week-old cohorts of non-HD controls (A), HD N171-82Q mice (B), and HD N171-82Q mice induced to express PGC-1α (C). Sections were stained with NeuN and visualized with diaminobenzidine. Scale bar for all sections is shown in panel C. CC = corpus callosum; FF = fimbria fornix

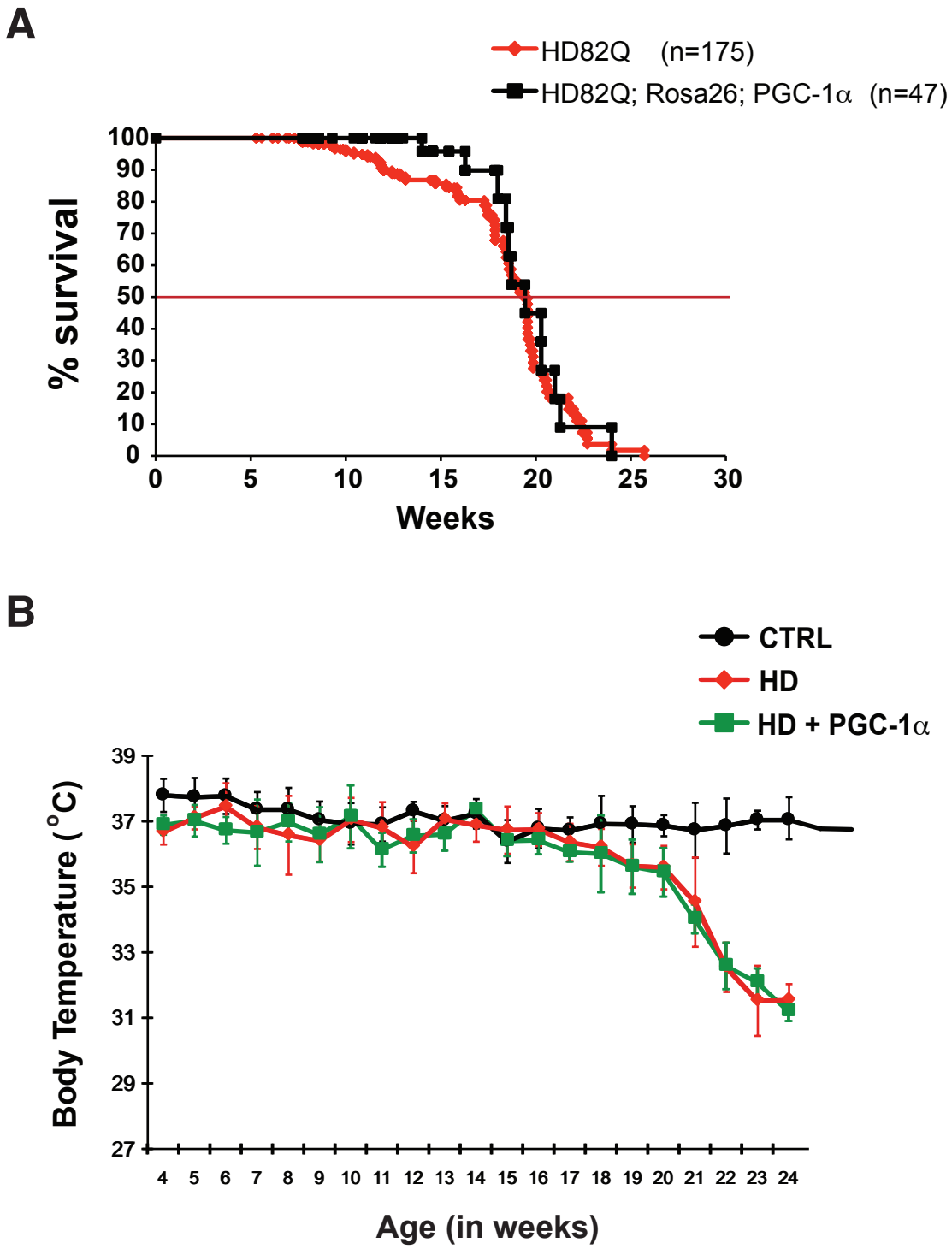

Figure S4. Effect of PGC-1α over-expression on HD mouse survival and thermoregulation

A) Kaplan-Meier analysis of HD N171-82Q mice (HD82Q) and Rosa26-rtTA – HD N171-82Q – TRE-PGC-1α triple transgenic mice (HD82Q; Rosa26; PGC-1α) reveals extended survival for HD mice over-expressing PGC-1α during the first 20 weeks of life ($p < .05$). However, after roughly half of the cohort have succumbed to disease, the remainder of the triple transgenic cohort do not exhibit any survival benefit, despite being in the PGC-1α over-expression group, resulting in no overall extension in lifespan.
B) We measured body temperature for cohorts (n = 12 – 14 / group) of non-HD controls (CTRL), HD N171-82Q mice (HD), and HD N171-82Q mice induced to express PGC-1α (HD + PGC-1α) for their entire lifespan. Beginning at 19 weeks of age, HD mice display a significant reduction in body temperature, which progressively worsens until they succumb to their disease. HD mice induced to over-express PGC-1α display an almost identical progressive reduction in body temperature, also beginning at 19 weeks of age and persisting until the time of their death.

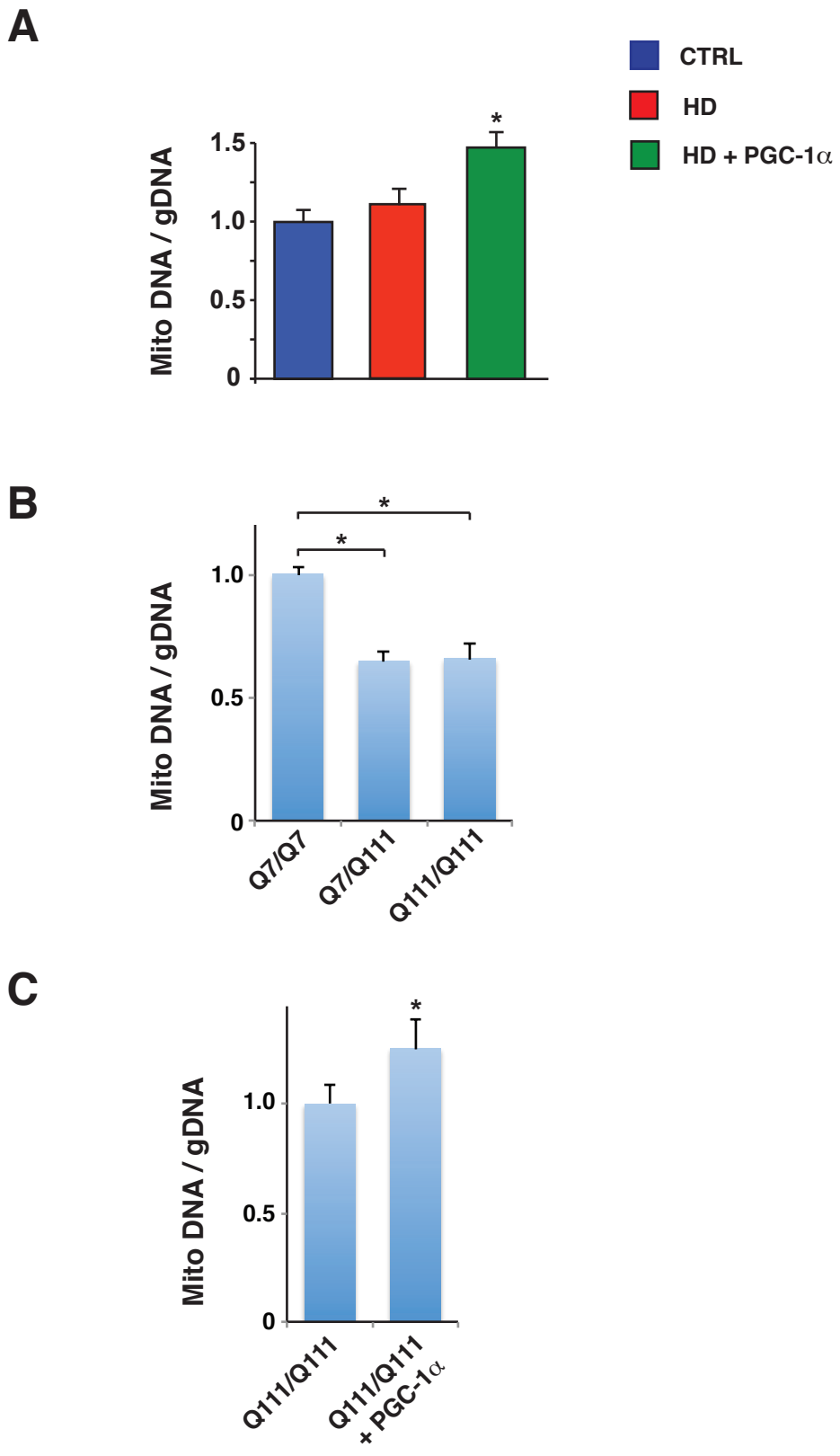

Figure S5. Mitochondrial DNA copy number is reduced in HD mice and striatal-like cells.

A) Real-time PCR analysis of striatal DNAs, obtained from sets (n = 3 / group) of 13 week-old HD mice, reveals that copy number of mitochondrial DNA, upon normalization to genomic DNA, is markedly increased in HD mice expressing PGC-1α (* $P < .05$). Error bars = s.e.m.

B) We quantified mitochondrial DNA copy number in ST-Hdh striatal-like cells, and observed significant reductions in mitochondrial DNA copy number, upon normalization to genomic DNA, in both Q7/Q111 cells and Q111/Q111 cells in comparison to Q7/Q7 cells (* $P < .05$). Error bars = s.e.m.

C) When we co-transfected Q111/Q111 ST-Hdh striatal-like cells with the PGC-1α expression construct, we observed a marked increase in mitochondrial DNA copy number (* $P < .05$). Error bars = s.e.m.

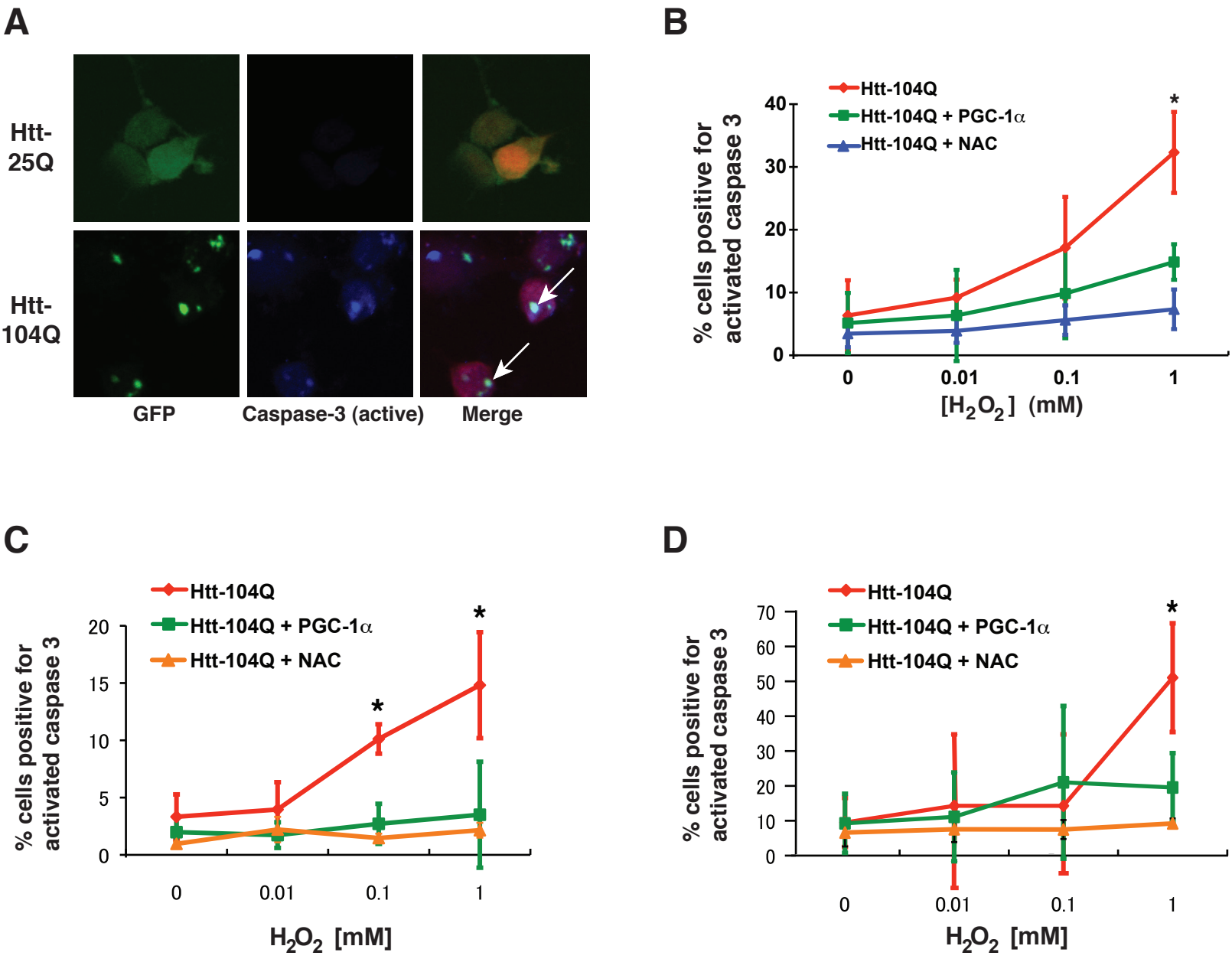

Figure S6. Effect of PGC-1α over-expression on cell death in htt-82Q-expressing cells

A) Expression of polyQ-expanded htt (Htt-104Q) in Neuro2a cells, cultured in 1 mM hydrogen peroxide, results in toxicity and cell death, based upon caspase-3 activation, as shown here. Expression of normal Q length htt (Htt-25Q) in Neuro2a cells, even in 1 mM hydrogen peroxide, does not elicit aggregate formation or toxicity.
B) We quantified neurotoxicity and cell death in Neuro2a cells expressing htt-104Q in the presence of RFP-empty vector, RFP-PGC-1α, or the reactive oxygen species scavenger NAC. Based upon immunostaining for active caspase-3, we found that htt-104Q expressing cells, that simultaneously express PGC-1α, or are exposed to NAC, display decreased levels of cell death in 1 mM hydrogen peroxide (* $P < .05$). Error bars = s.d.
C) Based upon immunostaining for active caspase-3 in htt-82Q expressing cells lacking visible aggregates, we found that htt-82Q expressing cells, that simultaneously express PGC-1α, or are exposed to NAC, display decreased levels of cell death in 0.1 mM and 1 mM hydrogen peroxide (* $P < .05$). Error bars = s.d.
D) Based upon immunostaining for active caspase-3 in htt-82Q expressing cells containing visible aggregates, we found that htt-82Q expressing cells, that simultaneously express PGC-1α, or are exposed to NAC, display decreased levels of cell death in 1 mM hydrogen peroxide (* $P < .05$). Error bars = s.d.

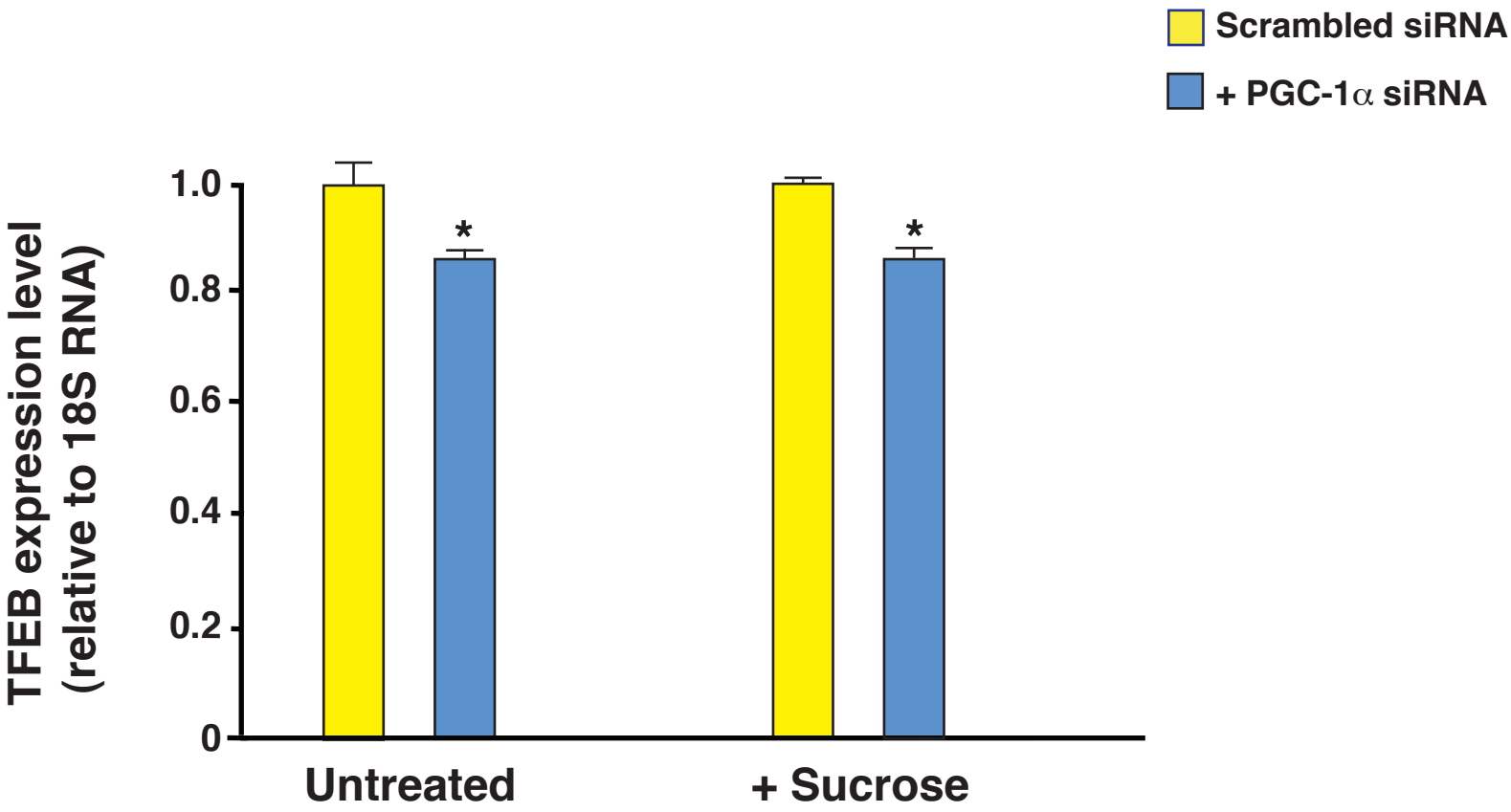

Figure S7. PGC-1α knock-down represses TFEB gene expression.

We transfected Neuro2a cells with a scrambled siRNA or a siRNA directed against PGC-1α, and we measured the expression level of TFEB in untreated cells or sucrose-treated cells at 48 hrs. PGC-1α knock-down of 40 – 50% was attained, and resulted in a significant reduction in TFEB RNA expression at baseline, or under lysosomal stress conditions (* $P < .05$). Error bars = s.e.m.

Supplementary References

S1. S. Gines, I.S. Seong, E. Fossale, E. Ivanova, F. Trettel, J.F. Gusella, V.C. Wheeler, F. Persichetti, M.E. MacDonald, Specific progressive cAMP reduction implicates energy deficit in presymptomatic Huntington's disease knock-in mice. *Hum Mol Genet* **12**, 497-508 (2003).

S2. J.E. Young, G.A. Garden, R.A. Martinez, F. Tanaka, C.M. Sandoval, A.C. Smith, B.L. Sopher, A. Lin, K.H. Fischbeck, L.M. Ellerby, R.S. Morrison, J.P. Taylor, A.R. La Spada, Polyglutamine-expanded androgen receptor truncation fragments activate a Bax-dependent apoptotic cascade mediated by DP5/Hrk. *J Neurosci* **29**, 1987-1997 (2009).

S3. K.J. Livak, S.J. Flood, J. Marmaro, W. Giusti, K. Deetz, Oligonucleotides with fluorescent dyes at opposite ends provide a quenched probe system useful for detecting PCR product and nucleic acid hybridization. *PCR Methods Appl* **4**, 357-362. (1995).

S4. A.R. La Spada, Y. Fu, B.L. Sopher, R.T. Libby, X. Wang, L.Y. Li, D.D. Einum, J. Huang, D.E. Possin, A.C. Smith, R.A. Martinez, K.L. Koszdin, P.M. Treuting, C.B. Ware, J.B. Hurley, L.J. Ptacek, S. Chen, Polyglutamine-expanded ataxin-7 antagonizes CRX function and induces cone-rod dystrophy in a mouse model of SCA7. *Neuron* **31**, 913-927. (2001).

S5. G.A. Garden, R.T. Libby, Y.H. Fu, Y. Kinoshita, J. Huang, D.E. Possin, A.C. Smith, R.A. Martinez, G.C. Fine, S.K. Grote, C.B. Ware, D.D. Einum, R.S. Morrison, L.J. Ptacek, B.L. Sopher, A.R. La Spada, Polyglutamine-expanded ataxin-7 promotes non-cell-autonomous purkinje cell degeneration and displays proteolytic cleavage in ataxic transgenic mice. *J Neurosci* **22**, 4897-4905. (2002).

S6. R. Kayed, E. Head, J.L. Thompson, T.M. McIntire, S.C. Milton, C.W. Cotman, C.G. Glabe, Common structure of soluble amyloid oligomers implies common mechanism of pathogenesis. *Science* **300**, 486-489 (2003).

S7. L. Chakrabarti, R. Zahra, S.M. Jackson, P. Kazemi-Esfarjani, B.L. Sopher, A.G. Mason, T. Toneff, S. Ryu, S. Shaffer, J.W. Kansy, J. Eng, G. Merrihew, M.J. MacCoss, A. Murphy, D.R. Goodlett, V. Hook, C.L. Bennett, L.J. Pallanck, A.R. La Spada, Mitochondrial dysfunction in NnaD mutant flies and Purkinje cell degeneration mice reveals a role for Nna proteins in neuronal bioenergetics. *Neuron* **66**, 835-847.

S8. E.R. Lazarowski, R. Tarran, B.R. Grubb, C.A. van Heusden, S. Okada, R.C. Boucher, Nucleotide release provides a mechanism for airway surface liquid homeostasis. *J Biol Chem* **279**, 36855-36864 (2004).

S9. K. Saijo, B. Winner, C.T. Carson, J.G. Collier, L. Boyer, M.G. Rosenfeld, F.H. Gage, C.K. Glass, A Nurr1/CoREST pathway in microglia and astrocytes protects dopaminergic neurons from inflammation-induced death. *Cell* **137**, 47-59 (2009).

S10. T.E. Anthony, C. Klein, G. Fishell, N. Heintz, Radial glia serve as neuronal progenitors in all regions of the central nervous system. *Neuron* **41**, 881-890 (2004).